

## ORIGINAL ARTICLE

# Effects of quaternary ammonium chain length on the antibacterial and remineralizing effects of a calcium phosphate nanocomposite

Ke Zhang<sup>1,2</sup>, Lei Cheng<sup>2,3</sup>, Michael D Weir<sup>2</sup>, Yu-Xing Bai<sup>1</sup> and Hockin HK Xu<sup>2,4,5</sup>

Composites containing nanoparticles of amorphous calcium phosphate (NACP) remineralize tooth lesions and inhibit caries. A recent study synthesized quaternary ammonium methacrylates (QAMs) with chain lengths (CLs) of 3–18 and determined their effects on a bonding agent. This study aimed to incorporate these QAMs into NACP nanocomposites for the first time to simultaneously endow the material with antibacterial and remineralizing capabilities and to investigate the effects of the CL on the mechanical and biofilm properties. Five QAMs were synthesized: DMAPM (CL3), DMAHM (CL6), DMADDM (CL12), DMAHDM (CL16), and DMAODM (CL18). Each QAM was incorporated into a composite containing 20% NACP and 50% glass fillers. A dental plaque microcosm biofilm model was used to evaluate the antibacterial activity. The flexural strength and elastic modulus of nanocomposites with QAMs matched those of a commercial control composite ( $n = 6$ ;  $P > 0.1$ ). Increasing the CL from 3 to 16 greatly enhanced the antibacterial activity of the NACP nanocomposite ( $P < 0.05$ ); further increasing the CL to 18 decreased the antibacterial potency. The NACP nanocomposite with a CL of 16 exhibited biofilm metabolic activity and acid production that were 10-fold lesser than those of the control composite. The NACP nanocomposite with a CL of 16 produced 2-log decreases in the colony-forming units (CFU) of total microorganisms, total streptococci, and mutans streptococci. In conclusion, QAMs with CLs of 3–18 were synthesized and incorporated into an NACP nanocomposite for the first time to simultaneously endow the material with antibacterial and remineralization capabilities. Increasing the CL reduced the metabolic activity and acid production of biofilms and caused a 2-log decrease in CFU without compromising the mechanical properties. Nanocomposites exhibiting strong anti-biofilm activity, remineralization effects, and mechanical properties are promising materials for tooth restorations that inhibit caries.

*International Journal of Oral Science* (2016) 8, 45–53; doi:10.1038/ijos.2015.33; published online 27 November 2015

**Keywords:** antibacterial nanocomposite; calcium phosphate nanoparticles; caries inhibition; human saliva microcosm biofilm; quaternary ammonium chain length

## INTRODUCTION

Many recent studies have indicated the worldwide prevalence of dental caries, which is a biofilm-dependent oral disease.<sup>1–2</sup> Due to their aesthetics and direct-filling capability, resin composites along with bonding agents are the principal materials for tooth cavity restorations.<sup>3–8</sup> However, composites tend to accumulate more biofilm than other restorative materials,<sup>9</sup> and secondary caries at the restoration margins promoted by acid production from biofilms is a major cause of composite restoration failure.<sup>10–12</sup> Therefore, the development of composites that can fight biofilms has become increasingly necessary.<sup>13</sup> To this end, quaternary ammonium methacrylates (QAMs) have been developed and incorporated into dental resins that exhibit anti-biofilm activities.<sup>14–21</sup>

Quaternary ammonium materials can cause bacteria lysis by binding to the bacterial membranes.<sup>22</sup> A previous study revealed that hydrophobic, positively charged long polymeric chains can effectively kill bacteria.<sup>23</sup> Furthermore, the alkyl chain length (CL) directly correlated with the hydrophobicity and consequently the ability to penetrate the hydrophobic bacterial membrane.<sup>24</sup> Specifically, these long cationic polymers can penetrate bacterial cells similar to the way a needle can burst a balloon.<sup>24–25</sup> Therefore, the CL of QAMs is important. A recent study synthesized a series of new QAMs with CLs ranging from 3 to 18, incorporated them into a bonding agent, and achieved strong antibacterial efficacy.<sup>26</sup> However, the effects of the CL on the antibacterial efficacy of dental composites have not yet been systematically studied.

<sup>1</sup>Department of Orthodontics, School of Stomatology, Capital Medical University, Beijing, China; <sup>2</sup>Biomaterials & Tissue Engineering Division, Department of Endodontics, Periodontics and Prosthodontics, School of Dentistry, University of Maryland, Baltimore, USA; <sup>3</sup>State Key Laboratory of Oral Diseases, West China Hospital of Stomatology, Sichuan University, Chengdu, China; <sup>4</sup>Center for Stem Cell Biology & Regenerative Medicine, School of Medicine, University of Maryland, Baltimore, USA and <sup>5</sup>Department of Mechanical Engineering, University of Maryland, Baltimore County, USA

Correspondence: Professor HHK Xu, Biomaterials & Tissue Engineering Division, Department of Endodontics, Periodontics and Prosthodontics, Dental School, University of Maryland, Baltimore MD 21201, USA

E-mail: hxu@umaryland.edu

Professor YX Bai, Department of Orthodontics, School of Stomatology, Capital Medical University, Beijing 100050, China

E-mail: byuxing@263.net

Accepted 3 August 2015

In addition to endowing composites with antibacterial activity, calcium phosphate (CaP) dental composites have also been employed to combat caries. CaP biomaterials are important because they are similar to the minerals in natural enamel and dentin. Dental resins containing CaP filler particles were shown to release calcium (Ca) and phosphate (P) ions, which were able to remineralize tooth lesions.<sup>27–28</sup> Traditional CaP composites contained CaP fillers with particle sizes of approximately 1–55  $\mu\text{m}$ .<sup>27–28</sup> However, these materials exhibit relatively low mechanical strengths, making them inadequate for use in stress-bearing areas or as bulk restoratives.<sup>27,29</sup> Recently, novel nanoparticles of amorphous calcium phosphate (NACP) have been developed, and the mechanical strength of the NACP nanocomposite was twofold to threefold higher than those of traditional CaP composites.<sup>30</sup> These nanoparticles can release cavity-fighting ions and neutralize acids.<sup>31</sup> Furthermore, novel NACP nanocomposites effectively remineralized enamel lesions *in vitro*<sup>32</sup> and greatly reduced caries formation at the composite-enamel margins in a human *in situ* model.<sup>33</sup>

To further enhance their caries-inhibiting capability, QAMs were mixed with an NACP nanocomposite to endow the material with both antibacterial and remineralizing capabilities.<sup>34</sup> The resultant NACP–QAM nanocomposite greatly decreased biofilm growth and exhibited constant antibacterial activity for up to 6 months of water-aging, indicating long-term durability.<sup>34</sup> Another study compared dimethylaminohexane methacrylate (DMAHM) with a CL of 6 to dimethylaminododecyl methacrylate (DMADDM) with a CL of 12 in an NACP nanocomposite and found that DMADDM was much more antibacterial than DMAHM.<sup>35</sup> However, QAMs with other CL values have not yet been incorporated into NACP nanocomposites in order to establish the effect of CL on dental composites.

In this study, QAMs with CLs ranging from 3 to 18 were incorporated into an NACP composite in order to establish the effect of CL on the antibacterial potency of the dental composite and to develop an NACP–QAM nanocomposite that exhibits both remineralization and potent antibacterial activity. Three hypotheses were tested: (i) a strong antibacterial NACP nanocomposite can be developed without sacrificing the mechanical properties of the material; (ii) the antibacterial potency of the NACP composite will directly correlate with the CL; and (iii) the optimal CL will significantly reduce both the acid produced by dental plaque microcosm biofilms and the colony-forming units (CFU) by several orders of magnitude.

## MATERIALS AND METHODS

### Synthesis of new QAMs with different CL

A series of new QAMs were synthesized using a modified Menshutkin reaction method,<sup>18</sup> which proceeds by the addition reaction of a tertiary amine to an organo-halide.<sup>20,35</sup> The advantage of this method is that the reaction products are generated at virtually quantitative amounts and require no further purification.<sup>18</sup> To form a QAM, 2-(dimethylamino) ethyl methacrylate (DMAEMA) was selected as the methacrylate-containing tertiary amine. For example, to synthesize dimethylaminododecyl methacrylate (DMADDM) with a CL of 12, 10 mmol of DMAEMA, 10 mmol of 1-bromododecane (BDD; TCI America, Portland, OR, USA), and 3 g of ethanol were added to a vial, which was capped and stirred at 70 °C for 24 h.<sup>35–36</sup> After the reaction was completed, ethanol was removed *via* evaporation. This procedure yielded DMADDM as a clear and viscous liquid. The identities of the reaction and products were verified *via* Fourier transform infrared spectroscopy in previous studies.<sup>35–36</sup> Five QAMs with different CLs were synthesized and are listed in Table 1.

**Table 1** Synthesis of QAMs with various alkyl chain lengths

Tertiary amine	Alkyl organo-halide	Product	CL
2-(dimethylamino) ethyl methacrylate (DMAEMA)	1-Bromopropane (BP)	DMAPM	3
	1-Bromohexane (BH)	DMAHM	6
	1-Bromododecane (BDD)	DMADDM	12
	1-Bromohexadecane (BHD)	DMAHDM	16
	1-Bromooctadecane (BOD)	DMAODM	18

CL, chain length; DMAPM, dimethylaminopropyl methacrylate; DMAHM, dimethylaminohexyl methacrylate; DMADDM, dimethylaminododecyl methacrylate; DMAHDM, dimethylaminohexadecyl methacrylate; DMAODM, dimethylaminooctadecyl methacrylate.

### Synthesis of NACP

NACP [ $\text{Ca}_3(\text{PO}_4)_2$ ] nanoparticles were synthesized using a spray-drying technique as described elsewhere.<sup>30</sup> Briefly, calcium carbonate ( $\text{CaCO}_3$ ; Fisher, Fair Lawn, NJ, USA) and anhydrous dicalcium phosphate ( $\text{CaHPO}_4$ ; Baker Chemical, Phillipsburg, NJ, USA) were dissolved in acetic acid to yield Ca and P concentrations of 8 and 5.333  $\text{mmol}\cdot\text{L}^{-1}$ , respectively, and a Ca/P molar ratio of 1.5. This solution was sprayed into a heated chamber, and an electrostatic precipitator (Air Quality, Minneapolis, MN, USA) collected the dried particles. This method produced NACP nanoparticles with a mean particle size of 116 nm and a particle size range from approximately 10 to 300 nm.<sup>30</sup>

### Fabrication of QAM–NACP nanocomposite

Bisphenol A glycidyl dimethacrylate (BisGMA) and triethylene glycol dimethacrylate (TEGDMA; Esstech, Essington, PA, USA) were mixed at a mass ratio of 1:1. Subsequently, 0.2% camphorquinone and 0.8% ethyl 4-N,N-dimethylaminobenzoate were added to allow the BisGMA–TEGDMA resin to be cured by light (referred to as BT). A QAM was mixed with BT at a QAM/(BT + QAM) mass fraction of 10%, as indicated in previous studies.<sup>20,26,35</sup> The resin was then mixed with 20% NACP and 50% glass particles, yielding a cohesive paste.<sup>30</sup> The glass particles consisted of barium borosilicate with a median size of 1.4  $\mu\text{m}$  (Caulk/Dentsply, Milford, DE, USA), and these particles were silanized with 4% 3-methacryloxypropyltrimethoxysilane and 2% n-propylamine. Because the resin mass fraction was 30%, the QAM mass fraction in the overall composite was 3%. A commercial composite served as a control (Renamel; Cosmedent, Chicago, IL, USA). Renamel consists of 60% nanofillers with a particle size of 20–40 nm in a methacrylate-ester resin. The BT resin (no QAM) containing 20% NACP and 50% silanized glass particles served as the NACP nanocomposite control.

Therefore, seven composites were tested: five NACP–QAM composites incorporating the five different QAMs listed in Table 1, a commercial composite control, and an NACP nanocomposite control. For mechanical testing, each paste was placed into rectangular molds of 2 mm  $\times$  2 mm  $\times$  25 mm. For biofilm experiments, each paste was placed into disk molds of 9 mm diameter and 2 mm thickness. The specimens were photo-cured (Triad 2000; Dentsply, York, PA, USA) for 1 min on each open side and then incubated in distilled water at 37 °C for 24 h prior to mechanical or biofilm testing.

### Mechanical testing

The specimens were tested using a computer-controlled Universal Testing Machine (5500R; MTS, Cary, NC, USA) in three-point flexure with a span of 10 mm at a crosshead speed of 1  $\text{mm}\cdot\text{min}^{-1}$ . The flexural strength,  $S$ , was calculated as follows:

$$S = 3P_{\max}L/(2bh^2)$$

where  $P_{\max}$  is the load-at-failure,  $L$  is the span,  $b$  is the specimen width, and  $h$  is the specimen thickness. The elastic modulus,  $E$ , was calculated as follows:

$$E = (P/d)(L^3/[4bh^3])$$

where  $P$  is the load,  $d$  is the displacement, and their ratio is the slope in the linear elastic region of the load-displacement curve. The specimens were taken out of the water and fractured within several minutes while still wet.<sup>30</sup>

#### Human saliva collection for dental plaque microcosm biofilm model

Whole human saliva was used as an inoculum to obtain multispecies biofilms consisting of organisms found in the oral cavity. The protocol was approved by the University of Maryland Baltimore Institutional Review Board.<sup>20,37</sup> Saliva is ideal for growing biofilms that maintain much of the complexity and heterogeneity observed *in vivo*.<sup>38</sup> Thus, saliva from 10 healthy individuals was collected and mixed for the experiments to maintain the diversity of bacterial populations.<sup>20,37</sup> All donors had natural dentition without active caries or periopathology and had not used antibiotics during the past three months. They did not brush their teeth for 24 h and fasted for at least 2 h before saliva collection.<sup>20,37</sup> Stimulated saliva was collected during parafilm chewing and kept on ice. An equal volume of saliva from each of the 10 donors was combined, then diluted in sterile glycerol to a concentration of 70% saliva and 30% glycerol, and stored at  $-80^{\circ}\text{C}$ .<sup>20,37</sup>

#### Live/dead biofilm staining

A growth medium was inoculated with the saliva-glycerol stock at a final dilution of 1:50. The growth medium contained  $2.5\text{ g}\cdot\text{L}^{-1}$  mucin (type II, porcine, gastric);  $2.0\text{ g}\cdot\text{L}^{-1}$  bacteriological peptone,  $2.0\text{ g}\cdot\text{L}^{-1}$  tryptone,  $1.0\text{ g}\cdot\text{L}^{-1}$  yeast extract,  $0.35\text{ g}\cdot\text{L}^{-1}$  NaCl,  $0.2\text{ g}\cdot\text{L}^{-1}$  KCl,  $\text{CaCl}_2$ ,  $0.1\text{ g}\cdot\text{L}^{-1}$  cysteine hydrochloride,  $0.001\text{ g}\cdot\text{L}^{-1}$  haemin, and  $0.2\text{ mg}\cdot\text{L}^{-1}$  vitamin  $\text{K}_1$  at pH 7.<sup>38</sup> Each composite disk was placed into a well of a 24-well plate. Each well was filled with 1.5 mL of inoculum and incubated in 5%  $\text{CO}_2$  at  $37^{\circ}\text{C}$ . After 8 h, each specimen was transferred to a well of a new 24-well plate with 1.5 mL fresh medium and was further incubated in 5%  $\text{CO}_2$  at  $37^{\circ}\text{C}$  for 16 h. Subsequently, each specimen was transferred into a well of a new 24-well plate with 1.5 mL fresh medium and incubated in 5%  $\text{CO}_2$  at  $37^{\circ}\text{C}$  for 24 h.<sup>20,37</sup> In total, the specimens were cultured for two days, which was sufficient to form microcosm biofilms on the resins.<sup>20,37</sup>

Disks with two-day biofilms were rinsed with phosphate-buffered saline (PBS) and live/dead stained using a BacLight live/dead bacterial viability kit (Molecular Probes, Eugene, OR, USA). Confocal scanning laser microscopy (CLSM 510; Carl Zeiss, Thornwood, NY, USA) was used to image the biofilms. Live bacteria were stained with Syto 9 to produce green fluorescence, and bacteria with compromised membranes were stained with propidium iodide to produce red fluorescence. Each specimen was photographed in four randomly selected fields of view, and three specimens per group were examined.

#### Biofilm metabolic activity measurement

Composite disks were inoculated with bacteria and cultured for two days as described above. The 2-day biofilms on each disk ( $n = 6$ ) were placed in 24-well plates, inoculated with 1 mL of 3-(4,5-dimethylthiazol-2-yl)-2,5-diphenyltetrazolium bromide (MTT) solution (with  $0.5\text{ g}\cdot\text{L}^{-1}$  MTT in PBS) at  $37^{\circ}\text{C}$  in 5%  $\text{CO}_2$  for 1 h.<sup>20,37</sup> During the incubation, metabolically active bacteria metabolized the MTT, a yellow tetrazole, and reduced it to purple formazan inside the living cells. The disks were then transferred to

new 24-well plates, and 1 mL of dimethyl sulfoxide (DMSO) was applied to solubilize the formazan crystals. The plates were incubated for 20 min with gentle mixing at room temperature. Two hundred microlitres of the DMSO solution from each well was collected, and its absorbance was measured at 540 nm using a microplate reader (SpectraMax M5; Molecular Devices, Sunnyvale, CA, USA). The absorbance directly correlated with the formazan concentration and consequently the metabolic activity in the biofilm on the surface of the composite.<sup>20,37</sup>

#### Lactic acid production by biofilms

Composite disks were inoculated with bacteria and cultured for two days as described above. The 2-day biofilms on the specimens ( $n = 6$ ) were rinsed with cysteine peptone water (CPW) to remove loosely attached bacteria and then transferred to 24-well plates containing 1.5 mL of buffered peptone water (BPW) plus 0.2% sucrose. The specimens were then incubated for 3 h to allow the biofilms to produce acid. The BPW solutions were then collected to analyze the lactate content using an enzymatic method.<sup>20,37</sup> Specifically, the BPW absorbance at 340 nm was measured using a microplate reader (SpectraMax M5), and standard curves were prepared using a lactic acid standard (Supelco Analytical, Bellefonte, PA, USA).<sup>20,37</sup>

#### Biofilm CFU counts

Disks covered with 2-day biofilms were transferred to tubes containing 2 mL CPW, and the biofilms were then harvested by sonication (3510R-MTH; Branson, Danbury, CT, USA) for 5 min, followed by vortexing at  $2400\text{ r}\cdot\text{min}^{-1}$  for 30 s using a vortex mixer (Fisher, Pittsburgh, PA, USA), as described in previous studies.<sup>20,37</sup> Three types of agar plates were used to assess the viability microorganisms after serial dilution in CPW. Tryptic soy blood agar culture plates were used to determine the viability of all microorganisms. Mitis salivarius agar (MSA) culture plates containing 15% sucrose were used to determine the viability of all streptococci, whereas MSA agar plates containing 0.2 units of bacitracin per mL were used to determine the viability of mutans streptococci. MSA contains selective agents that inhibit many species of bacteria but not streptococci, allowing streptococci to grow. MSA plus bacitracin may inhibit other species that constitute the oral microflora but does not affect cariogenic mutans streptococci, because of their resistance to bacitracin.<sup>20,35,37</sup>

#### Ca and P ion release from NACP composite containing CL16

The aforementioned tests demonstrated that the composite with a CL of 16 exhibited the strongest antibacterial activity. However, the effect of adding CL16 to the NACP composite on the Ca and P ion release capability was unknown. Therefore, the ions released by the NACP-CL16 composite and NACP composite control without CL16 were measured. A sodium chloride (NaCl) solution ( $133\text{ mmol}\cdot\text{L}^{-1}$ ) was buffered to three different pH values<sup>30,33</sup>: pH 4 with  $50\text{ mmol}\cdot\text{L}^{-1}$  lactic acid, pH 5.5 with  $50\text{ mmol}\cdot\text{L}^{-1}$  acetic acid, and pH 7 with  $50\text{ mmol}\cdot\text{L}^{-1}$  HEPES. Following previous studies<sup>30,33</sup>, three composite specimens of approximately  $2\text{ mm} \times 2\text{ mm} \times 12\text{ mm}$  were immersed in 50 mL of solution at each pH, yielding a specimen volume/solution of  $2.9\text{ mm}^3\cdot\text{mL}^{-1}$ . The concentrations of Ca and P released from the specimens were measured at 1, 3, 7, 14, 21, and 28 d. At each time point, aliquots of 0.5 mL were removed and replaced with fresh solution. The Ca and P ion concentrations of the aliquots were analyzed using the spectrophotometric method (DMS-80 UV-visible; Varian, Palo Alto, CA, USA) as well as known standards and calibration curves, as described previously.<sup>27–30,33</sup>

#### Statistical analysis

One-way and two-way analyses of variance were performed to detect the significant effects of the variables. Tukey's multiple comparison test was used to compare the data at  $P = 0.05$ .



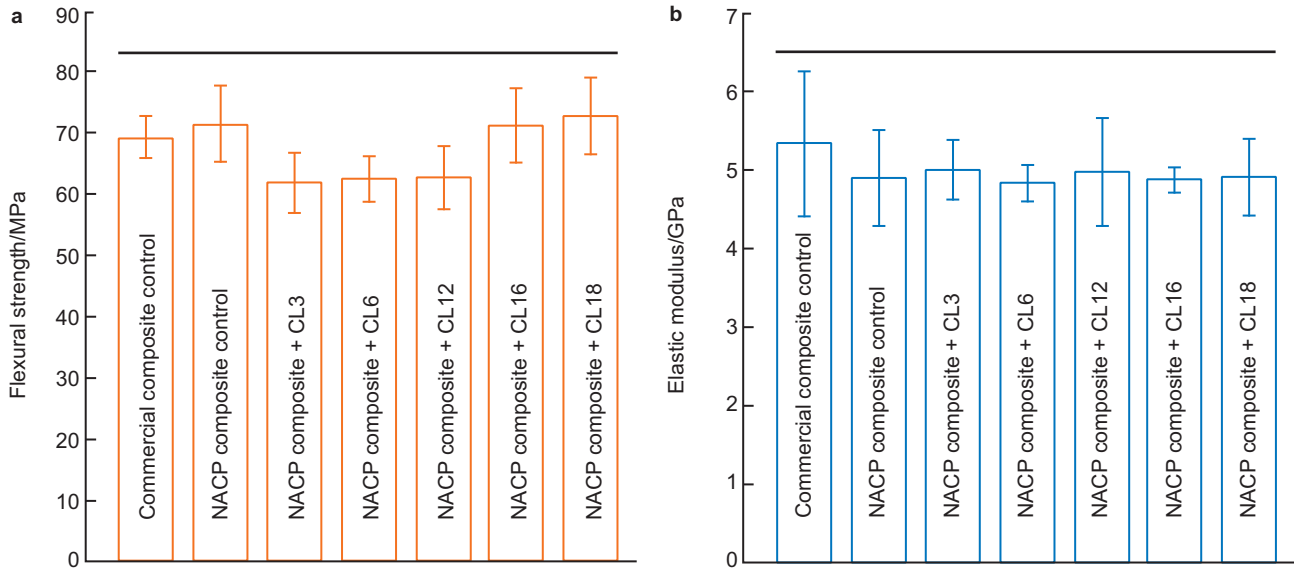


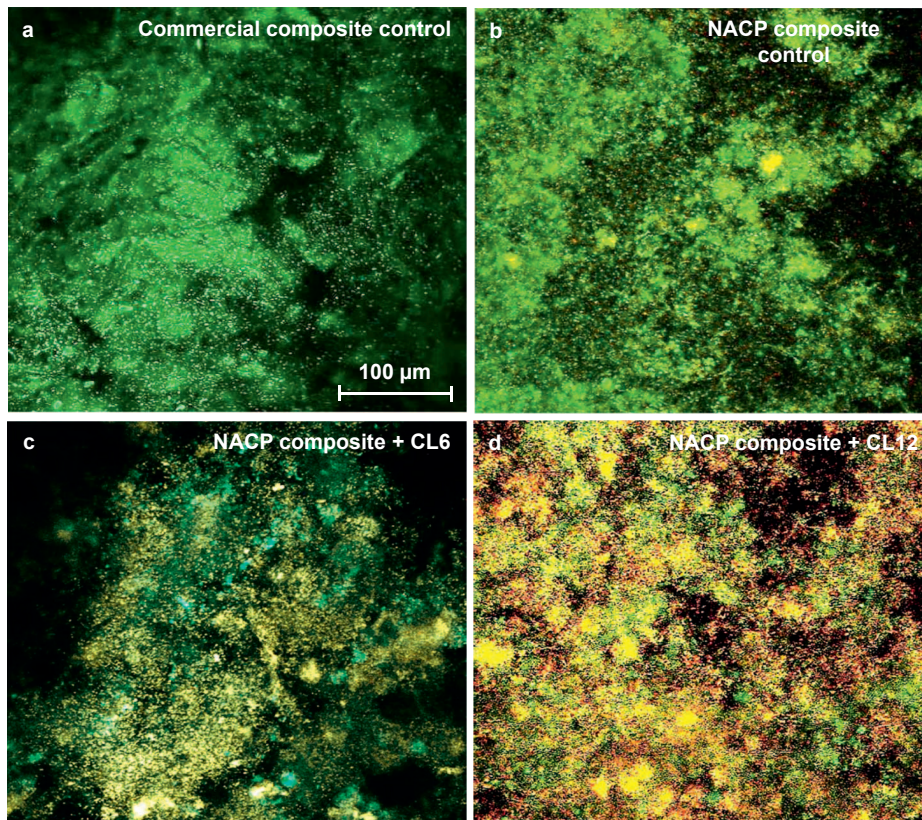
**Figure 1 Mechanical properties of composites.** (a) Flexural strength; (b) elastic modulus. Mean  $\pm$  SD;  $n = 6$ . The incorporation of QAMs with a CL ranging from 3 to 18 into NACP nanocomposite did not significantly decrease the strength and elastic modulus. Horizontal line indicates  $P > 0.1$ . CL, chain length; NACP, nanoparticles of amorphous calcium phosphate; QAM, quaternary ammonium methacrylates; SD, standard deviation.

## RESULTS

The mechanical properties of composites are plotted in Figure 1: (a) flexural strength and (b) elastic modulus (mean  $\pm$  standard deviation (SD);  $n = 6$ ). The flexural strengths of the composites did not significantly differ ( $P > 0.1$ ). Therefore, QAMs were incorporated into the NACP nanocomposite without compromising the mechanical strength.

The elastic moduli of the QAM–NACP nanocomposites were also similar to those of the two control groups ( $P > 0.1$ ).

Figure 2 shows the representative CLSM images of live/dead stained biofilms adherent on the composites: (a) commercial composite control, (b) NACP nanocomposite control, (c) NACP nanocomposite containing CL6 (as listed in Table 1), (d) NACP nanocomposite containing



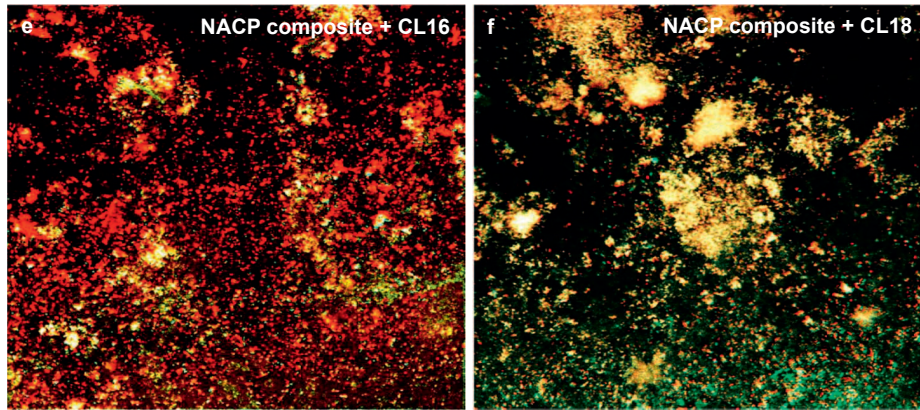


**Figure 2** Representative CLSM images of live/dead stained biofilms grown for two days on composites. The material name is indicated in each image, and the magnification of all images is the same as that in **a**. Live bacteria were stained green, and dead bacteria were stained red. Live and dead bacteria that co-localized appeared yellow or orange. Commercial composite and NACP nanocomposite without QAM had primarily live bacteria. Increasing the CL enhanced the antibacterial activity, with CL16 producing mostly red and orange staining. CL, chain length; NACP, nanoparticles of amorphous calcium phosphate; QAM, quaternary ammonium methacrylates.

CL12, (e) NACP nanocomposite containing CL16, and (f) NACP nanocomposite containing CL18. The live/dead images of the NACP nanocomposite containing CL3 were similar to that of (b) and are not included here. Live bacteria were stained green, and dead bacteria were stained red. Yellow or orange indicated co-localized live and compromised bacteria. Biofilms on the two controls without QAM were primarily covered in live bacteria, whereas some dead bacteria started to appear in (c). This proportion of dead bacteria increased on (d), and the biofilm on (e) was primarily dead. These results demonstrate that increasing the CL of QAM in the NACP nanocomposite enhanced the antibacterial activity, which reached maximum potency at CL16. Further increasing the CL to 18 appeared to decrease the antibacterial potency compared with CL16, as indicated by some live bacteria in the biofilms on the NACP nanocomposite containing CL18.

The metabolic activity results from the MTT assay of biofilms adherent on the composites are plotted in Figure 3 (mean  $\pm$  SD;  $n = 6$ ). The biofilms on the commercial composite and NACP composite without

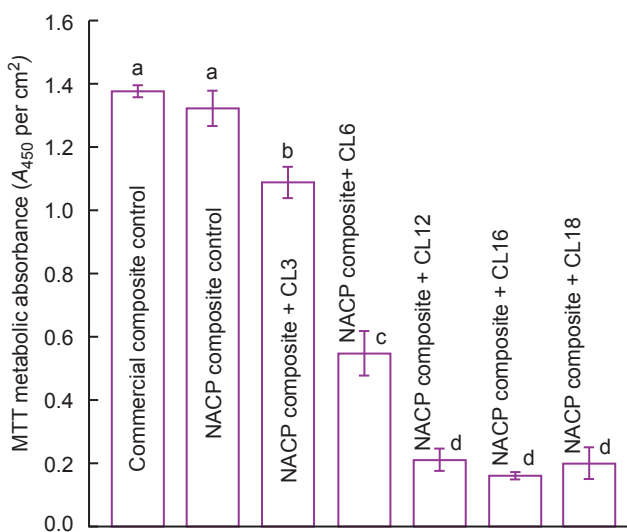
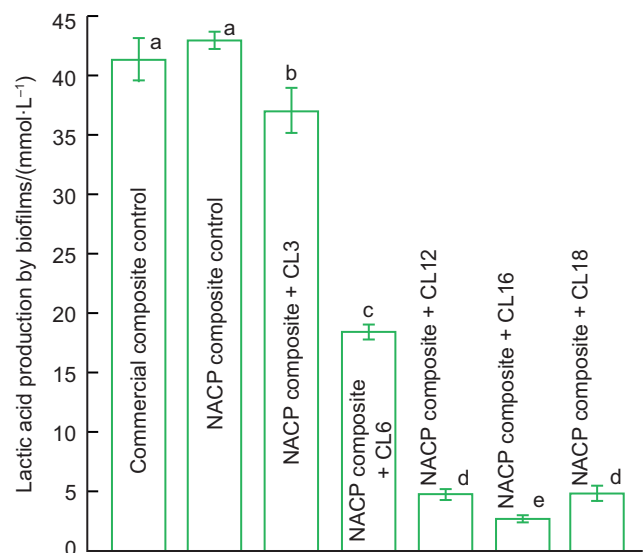


**Figure 3** MTT metabolic activity of 2-day biofilms covering the composites. Mean  $\pm$  SD;  $n = 6$ . Values with dissimilar letters are significantly different from each other ( $P < 0.05$ ). CL, chain length; MTT, 3-(4,5-dimethylthiazol-2-yl)-2,5-diphenyltetrazolium bromide; NACP, nanoparticles of amorphous calcium phosphate; SD, standard deviation.

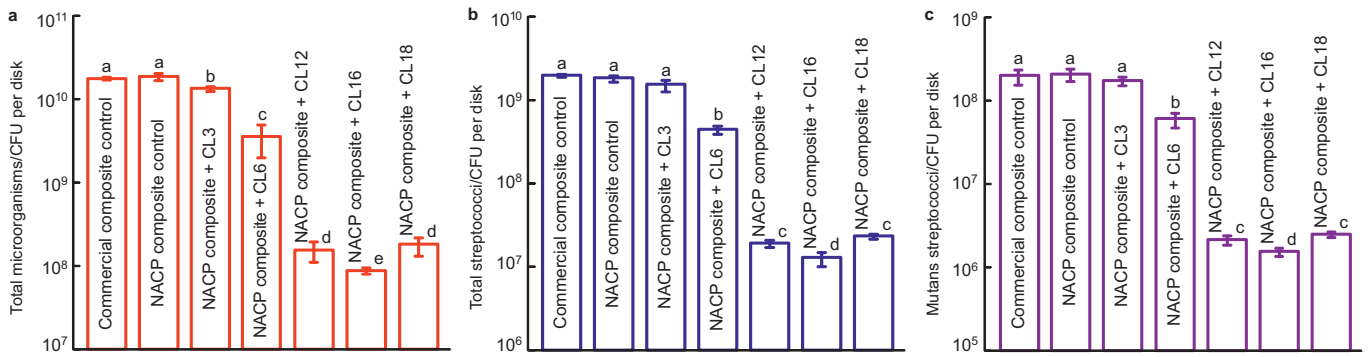
QAM exhibited similar metabolic activity ( $P > 0.1$ ). Increasing the CL from 3 to 18 significantly decreased the metabolic activity of biofilms ( $P < 0.05$ ), and a CL of 16 minimized the metabolic activity. Further increasing the CL to 18 did not further decrease the metabolic activity compared with a CL of 16 ( $P > 0.1$ ).

Figure 4 plots the lactic acid production of biofilms adherent to the composites (mean  $\pm$  SD;  $n = 6$ ). The biofilms on the two control composites produced the most acid. Increasing the CL from 3 to 16 significantly decreased the acid production capability of the biofilms ( $P < 0.05$ ), and a CL of 16 minimized lactic acid production ( $P < 0.05$ ). Specifically, the lactic acid production of the biofilm on the nanocomposite with a CL of 16 was 10-fold less than the production of films on the control composites.

The 2-day biofilm CFU counts per composite disk are plotted in Figure 5 for: (a) total microorganisms, (b) total streptococci, and (c) mutans streptococci. (mean  $\pm$  SD;  $n = 6$ ). In each plot, the two control



**Figure 4** Lactic acid production by 2-day biofilms adherent on composites. Mean  $\pm$  SD;  $n = 6$ . Values with dissimilar letters are significantly different from each other ( $P < 0.05$ ). CL, chain length; NACP, nanoparticles of amorphous calcium phosphate; SD, standard deviation.



**Figure 5** CFU counts of 2-day biofilms on composites. (a) Total microorganisms; (b) total streptococci; (c) mutans streptococci. Mean  $\pm$  SD;  $n = 6$ . In each plot, values with dissimilar letters are significantly different from each other ( $P < 0.05$ ). The two control composites exhibited the highest CFU counts. Increasing the CL from 3 to 16 significantly decreased the CFU counts ( $P < 0.05$ ). Note the log scale for the  $y$ -axis. CFU, colony-forming unit; CL, chain length; NACP, nanoparticles of amorphous calcium phosphate; SD, standard deviation.

composites yielded the highest CFU counts. Increasing the CL from 3 to 16 enhanced the antibacterial activity, as evidenced by significantly decreased CFU counts ( $P < 0.05$ ). For QAM CLs in the NACP nanocomposites ranging from 3 to 16, the CFU inversely correlated with the CL; however, at CL18, the antibacterial activity was not as strong as that

observed at CL16. Compared with the control composites, all three CFU counts were reduced by two orders of magnitude on the NACP nanocomposite containing CL16.

The Ca and P ion releases are plotted in Figure 6 (mean  $\pm$  SD;  $n = 4$ ): (a) Ca ion release for NACP composite, (b) Ca ion release for NACP

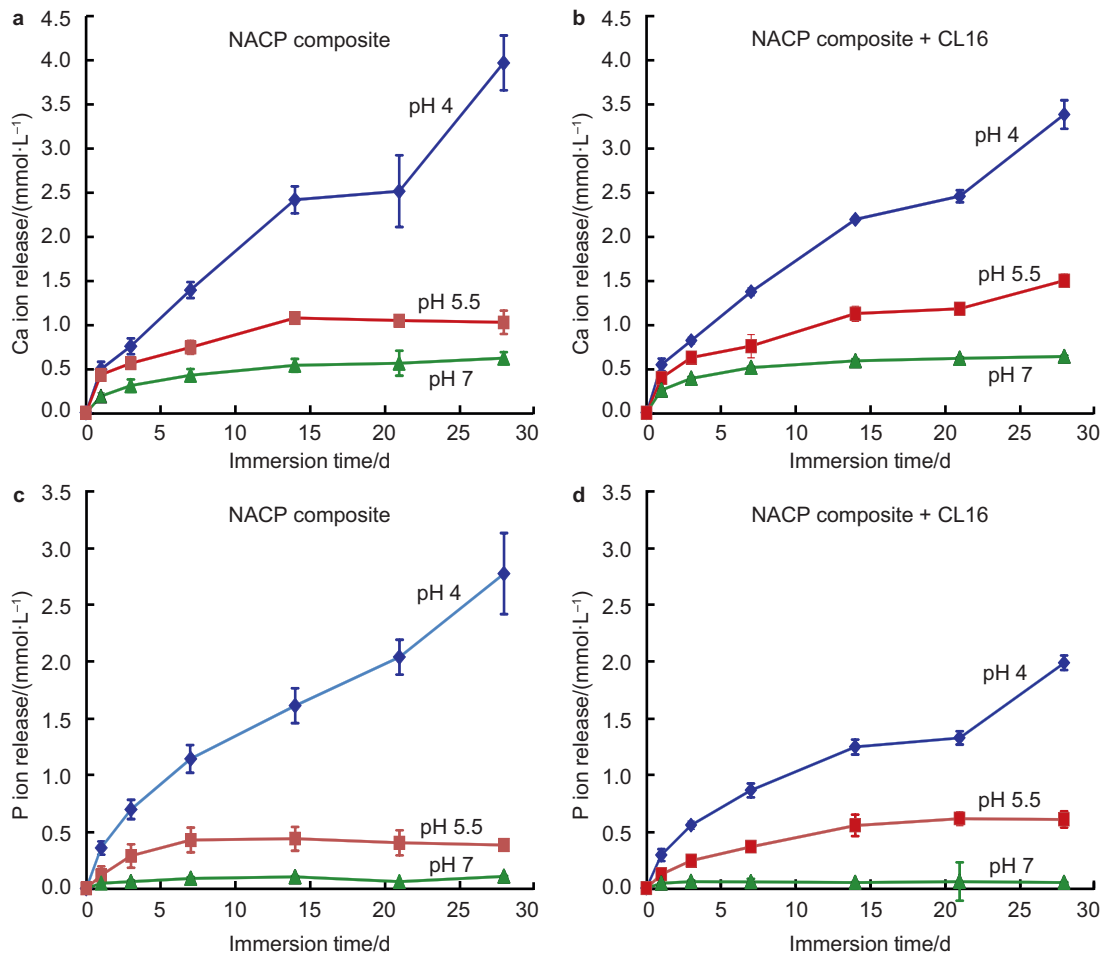


**Figure 6** Calcium (Ca) and phosphate (P) ion release from NACP composite and NACP composite containing CL16. (a) Ca ion release for NACP composite; (b) Ca ion release for NACP composite with a CL of 16; (c) P ion release for NACP composite; (d) P ion release for NACP composite with a CL of 16. Mean  $\pm$  SD;  $n = 4$ . The cumulative concentrations of released ions are reported. The experiments were performed at three different pH values of 4, 5.5, and 7 to simulate the different plaque pH levels *in vivo*. The ion release increased dramatically at a cariogenic pH of 4, when such ions are most needed to combat tooth demineralization. CL, chain length; NACP, nanoparticles of amorphous calcium phosphate; SD, standard deviation.



composite with CL16, (c) P ion release for NACP composite, and (d) P ion release for NACP composite with CL16. Specifically, the pH inversely correlated with the ion release ( $P < 0.05$ ). For example, at pH 4 and 28 d, the NACP composite containing a CL of 16 exhibited moderately lower Ca and P ion releases than the NACP composite ( $P < 0.05$ ).

## DISCUSSION

The present study developed nanocomposites with double benefits of remineralization *via* NACP and antibacterial function *via* QAM, and determined the effects of CL from 3 to 18 on dental composites for the first time. The most potent composite, which contained NACP and DMAHDM with a CL of 16, significantly reduced the biofilm metabolic activity and acid production and reduced the number of biofilm CFU on the composite by two orders of magnitude compared with the control composite. Notably, these results were achieved without negatively affecting the composite mechanical properties. In other words, the load-bearing capability of the dental NACP–DMAHDM nanocomposite was similar to that of the commercial control composite, but the dental NACP–DMAHDM nanocomposite exhibited the added benefits of both remineralization and antibacterial properties. Thus, this novel composite constitutes a promising strategy to inhibit biofilms and caries.

Dental resins containing QAM possess positively charged quaternary amine  $N^+$  that can interact with the negatively charged cell membrane of bacteria, leading to membrane disruption and cytoplasmic leakage.<sup>22</sup> Long-chain quaternary ammonium compounds have been postulated to be especially effective due to their ability to insert into the bacterial membrane, which results in physical disruption and bacteria death.<sup>39</sup> For example, the antibacterial potency of glass ionomer materials directly correlated with the CLs.<sup>40</sup> Another study of bonding agents showed substantial decreases in biofilm growth and the number of CFU as the CL was increased from 3 to 16.<sup>26</sup> Furthermore, the thickness and live volume of three-dimensional biofilms that were also grown on bonding agents decreased as the CL was increased from 3 to 16.<sup>41</sup> The present study focused on the effect of the CL on the dental composite, which was not investigated in previous studies of the CL. We found that increasing the CL from 3 to 16 in a series of QAMs increased the antibacterial potency of the composite. The results also showed that by further increasing the CL to 18 decreased the antibacterial efficacy of the composite. This decrease may be attributed to the bending or curling of excessively long alkyl chains. These long chains may cover the positively charged quaternary ammonium groups to partially block their electrostatic interactions with the bacteria, which would reduce the antibacterial efficacy. These results suggest that an alkyl chain of 16 may be the critical point for the alkyl chain to extend without burying the quaternary ammonium sites on the composite. However, the mechanisms responsible for the strong effect of the QAM CL in the dental composite on the oral biofilm growth require further investigation.

Most previous antibacterial resin studies focused on bonding agents, with only a few studies on dental composites.<sup>10,13</sup> Moreover, the effect of the CL on composites that exhibit both antibacterial and remineralizing capabilities had not yet been established. Dental composites are gaining popularity as materials for filling tooth cavities.<sup>3,5,7</sup> However, secondary caries remains a primary reason for failure, and the replacement of failed restorations accounts for 50%–70% of all restorations placed.<sup>11–12</sup> Specifically, biofilms have been shown to preferentially accumulate on composites compared with other restoratives.<sup>9</sup> Therefore, new composites capable of reducing plaque build-up are urgently needed. To this end, an antibacterial monomer,

MDPB, has been copolymerized in a composite, which significantly decreased glucan synthesis and the growth of *S. mutans* on the composite surfaces without affecting the mechanical properties or polymerization conversion of the composite.<sup>10,23</sup> Another study developed an antibacterial fluoride-releasing composite that yielded a significant reduction in *S. mutans* biofilm growth.<sup>19</sup> Furthermore, nanoparticles of quaternary ammonium polyethyleneimine (QPEI) have been added to a composite that exhibited significant antibacterial activity against salivary bacteria *in vivo*.<sup>42</sup> A furanone-containing antibacterial composite that yielded 16%–68% reduction in *S. mutans* viability has also been made.<sup>17</sup> Nevertheless, the present study is unique because the composite not only exhibited strong antibacterial activity, as evidenced by reductions of two orders of magnitude in the number of biofilm CFU, but also contained NACP for Ca and P, which endowed the composite with ion release and remineralization capabilities. Moreover, this study investigated the effect of CLs ranging from 3 to 18 on the composite. Previous studies have demonstrated the effectiveness of the NACP nanocomposite in remineralizing tooth lesions and inhibiting caries in a human *in situ* model.<sup>32–33</sup> Furthermore, a recent animal study showed that the NACP nanocomposite is biocompatible *in vivo*, as evidenced by a lack of pulpal inflammation and a three fold increase in tertiary dentin formation compared with that of the control composite.<sup>43</sup> However, further studies are needed to investigate the *in vivo* anti-caries efficacy of the NACP nanocomposite containing a CL of 16.

Mechanical properties are important for the composite to survive chewing forces and other stresses in the mouth. Previous CaP-filled resins using traditional CaP filler particles of 1–55  $\mu\text{m}$  exhibited strengths of 20–50 MPa.<sup>27</sup> In addition, these previous CaP resins did not exhibit antibacterial activity. Conversely, the NACP nanocomposite of the present study with a CL of 16 exhibited strong antibacterial activity and reached a flexural strength of 70 MPa. This strength matched that of a commercial control composite that lacked antibacterial and remineralizing capabilities. The small NACP particle size of 112 nm likely contributed to the improved mechanical properties of the composite.<sup>30</sup> These results are consistent with those of a previous study that showed that the three-body wear of an NACP nanocomposite after  $4 \times 10^5$  wear cycles was within the range of commercial controls. Furthermore, the strength of the NACP nanocomposite after two years of water-aging was moderately higher than that of the control composite and much higher than that of the resin-modified glass ionomers.<sup>44</sup> These mechanical properties should allow the NACP nanocomposite with a CL of 16 to be used in a variety of tooth cavity restorations.

The NACP composite with CL16 had moderately lower concentrations of Ca and P ions at 28 d and pH 4 than NACP composite without CL16. This reduction may be the result of ion exchange between the quaternary ammonium group in CL16 and the P ions from NACP.<sup>45</sup> CL16 was synthesized *via* a modified Menshutkin reaction by reacting a methacrylate-containing tertiary amine with 1-bromododecane. The resulting methacrylate contained the quaternary ammonium group  $(NR_4)^+$  as well as the  $Br^-$  counter-ion from the bromododecane. All QAMs synthesized in this manner contain the  $Br^-$  counter-ion. These  $Br^-$  ions are considered mobile and may be replaced by another ion of the same charge. Some of the P ions may have been exchanged with the mobile  $Br^-$  counter-ions, and these P ions were consequently trapped in the resin matrix and not released. This phenomenon may only be significant at a relatively high P ion concentration, which might explain the reduced P concentration at 28 d and a pH of 4. The much milder reduction in Ca

release from the NACP composite with a CL of 16 may be due to the lack of a direct effect of the quaternary ammonium group in CL16 on the Ca ions. Previous work suggested that P ions weakly chelate with Ca ions.<sup>46</sup> For the NACP composite containing CL16, the P ions trapped in the resin matrix may chelate with some of the Ca ions, which may slightly reduce the Ca release. Further studies are needed to investigate the effect of QAM on the ion release of dental restoratives.

The NACP nanocomposite containing QAM with a CL of 16 is promising for use in a wide range of dental composite restorations. In addition, it has potential for use in root caries restorations. As the world population ages and seniors retain an increasing number of their teeth, the incidence of tooth root caries is rapidly increasing in the elderly population.<sup>47</sup> These root caries result from gingival recession due to aging, excessive toothbrush use and abrasion, and periodontal diseases.<sup>47</sup> Moreover, two compounding reasons contribute to the high prevalence of root caries in seniors. First, seniors usually have relatively low salivary flow due to several reasons, such as xerostomia associated with certain medical conditions, polypharmacy, and atrophic changes in the glands. This low salivary flow may contribute to biofilm/plaque build-up because less saliva is available to neutralize the acid produced by biofilms.<sup>48</sup> Second, with gingival recession and root exposure in seniors, root minerals have a higher solubility and are less resistant to acid dissolution.<sup>49</sup> The tooth root is demineralized approximately twice as fast as enamel.<sup>50</sup> Therefore, the incidence of root caries has rapidly increased in the USA and positively correlates with age, ranging from 7% among young people to 56% in seniors 75 years of age or older.<sup>51</sup> The NACP nanocomposite with a CL of 16 could be useful in treating root caries. Specifically, the NACP may help to remineralize lesions and neutralize acids,<sup>31–33</sup> whereas the QAM with a CL of 16 may help to inhibit local biofilm growth and plaque accumulation. This material may also be employed for the minimally invasive management of dental caries,<sup>52</sup> for which the NACP may help to remineralize the residual lesions in the prepared tooth cavity. Further studies are needed to develop and optimize the NACP–DMAHDM nanocomposite for specific restorations.

## CONCLUSION

Novel antibacterial monomers with a series of alkyl CLs ranging from 3 to 18 were synthesized and incorporated into NACP nanocomposites to generate materials that exhibit both antibacterial function *via* the incorporation of an antibacterial monomer and remineralization *via* NACP. The alkyl CL of the antibacterial monomer in the NACP nanocomposite was shown to strongly affect antibacterial efficacy. Specifically, increasing the CL from 3 to 16 reduced the metabolic activity and lactic acid production of the dental plaque microcosm biofilms by 10-fold and decreased the CFU count of total microorganisms, total streptococci, and mutans streptococci by two orders of magnitude. The new antibacterial and remineralizing nanocomposite exhibited mechanical properties matching those of a commercial composite control that lacked antibacterial and remineralizing capabilities. Hence, the new nanocomposite, which exhibits potent anti-biofilm activity and remineralization capability, is a promising material for tooth cavity restorations that inhibit caries.

## ACKNOWLEDGEMENTS

We thank Drs XD Zhou, JM Antonucci, NJ Lin, S Lin-Gibson, and AF Fouad for the discussions and help. This study was supported by National Institutes of Health (NIH) R01DE17974 (Hockin HK Xu), National Natural Science

Foundation of China grant 81400540 (Ke Zhang), and a seed fund (Hockin HK Xu) from the University of Maryland School of Dentistry.

- 1 Bagramian RA, Garcia-Godoy F, Volpe AR. The global increase in dental caries. A pending public health crisis. *Am J Dent* 2009; **22**(1): 3–8.
- 2 Dye BA, Thornton-Evans G. Trends in oral health by poverty status as measured by healthy people 2010 objectives. *Public Health Rep* 2010; **125**(6): 817–830.
- 3 Drummond JL. Degradation, fatigue, and failure of resin dental composite materials. *J Dent Res* 2008; **87**(8): 710–719.
- 4 Ferracane JL. Buonocore lecture. Placing dental composites—a stressful experience. *Oper Dent* 2008; **33**(3): 247–257.
- 5 Spencer P, Ye Q, Park J *et al*. Adhesive/dentin interface: the weak link in the composite restoration. *Ann Biomed Eng* 2010; **38**(6): 1989–2003.
- 6 Pashley DH, Tay FR, Imazato S. How to increase the durability of resin-dentin bonds. *Compend Contin Educ Dent* 2011; **32**(7): 60–64, 66.
- 7 Ferracane JL. Resin composite—state of the art. *Dent Mater* 2011; **27**(1): 29–38.
- 8 Imazato S, Ma S, Chen JH *et al*. Therapeutic polymers for dental adhesives: loading resins with bio-active components. *Dent Mater* 2014; **30**(1): 97–104.
- 9 Beyth N, Domb AJ, Weiss EI. An *in vitro* quantitative antibacterial analysis of amalgam and composite resins. *J Dent* 2007; **35**(3): 201–206.
- 10 Imazato S, Torii M, Tsuchitani Y *et al*. Incorporation of bacterial inhibitor into resin composite. *J Dent Res* 1994; **73**(8): 1437–1443.
- 11 Sakaguchi RL. Review of the current status and challenges for dental posterior restorative composites: clinical, chemistry, and physical behavior considerations. Summary of discussion from the Portland Composites Symposium (POCOS) June 17–19, 2004, Oregon Health and Science University, Portland, Oregon. *Dent Mater* 2005; **21**(1): 3–6.
- 12 National Institute of Dental and Craniofacial Research (NIDCR). NIDCR announcement # 13-DE-102, *Dental resin composites and caries*. March 5, 2009.
- 13 Imazato S. Antibacterial properties of resin composites and dentin bonding systems. *Dent Mater* 2003; **19**(6): 449–457.
- 14 Ebi N, Imazato S, Noiri Y *et al*. Inhibitory effects of resin composite containing bactericide-immobilized filler on plaque accumulation. *Dent Mater* 2001; **17**(6): 485–491.
- 15 Li F, Chen J, Chai Z *et al*. Effects of a dental adhesive incorporating antibacterial monomer on the growth, adherence and membrane integrity of *Streptococcus mutans*. *J Dent* 2009; **37**(4): 289–296.
- 16 Li F, Chai ZG, Sun MN *et al*. Anti-biofilm effect of dental adhesive with cationic monomer. *J Dent Res* 2009; **88**(4): 372–376.
- 17 Weng Y, Howard L, Guo X *et al*. A novel antibacterial resin composite for improved dental restoratives. *J Mater Sci Mater Med* 2012; **23**(6): 1553–1561.
- 18 Antonucci JM, Zeiger DN, Tang K *et al*. Synthesis and characterization of dimethacrylates containing quaternary ammonium functionalities for dental applications. *Dent Mater* 2012; **28**(2): 219–228.
- 19 Xu X, Wang Y, Liao S *et al*. Synthesis and characterization of antibacterial dental monomers and composites. *J Biomed Mater Res Part B Appl Biomater* 2012; **100**(4): 1151–1162.
- 20 Cheng L, Zhang K, Melo MA *et al*. Anti-biofilm dentin primer with quaternary ammonium and silver nanoparticles. *J Dent Res* 2012; **91**(6): 598–604.
- 21 Zhang K, Cheng L, Wu EJ *et al*. Effect of water-ageing on dentine bond strength and anti-biofilm activity of bonding agent containing new monomer dimethylamino-dodecyl methacrylate. *J Dent* 2013; **41**(6): 504–513.
- 22 Beyth N, Yudovin-Farber I, Bahir R *et al*. Antibacterial activity of dental composites containing quaternary ammonium polyethylenimine nanoparticles against *Streptococcus mutans*. *Biomaterials* 2006; **27**(21): 3995–4002.
- 23 Lin J, Qiu S, Lewis K *et al*. Bactericidal properties of flat surfaces and nanoparticles derivatized with alkylated polyethylenimines. *Biotechnol Prog* 2002; **18**(5): 1082–1086.
- 24 Tiller JC, Liao CJ, Lewis K *et al*. Designing surfaces that kill bacteria on contact. *Proc Natl Acad Sci U S A* 2001; **98**(11): 5981–5985.
- 25 Murata H, Koepsel RR, Matyjaszewski K *et al*. Permanent, non-leaching antibacterial surface—2: how high density cationic surfaces kill bacterial cells. *Biomaterials* 2007; **28**(32): 4870–4879.
- 26 Li F, Weir MD, Xu HH. Effects of quaternary ammonium chain length on antibacterial bonding agents. *J Dent Res* 2013; **92**(10): 932–938.
- 27 Dickens SH, Flaim GM, Takagi S. Mechanical properties and biochemical activity of remineralizing resin-based Ca-PO<sub>4</sub> cements. *Dent Mater* 2003; **19**(6): 558–566.
- 28 Langhorst SE, O'Donnell JN, Skrtic D. *In vitro* remineralization of enamel by polymeric amorphous calcium phosphate composite: quantitative microradiographic study. *Dent Mater* 2009; **25**(7): 884–891.
- 29 Skrtic D, Antonucci JM, Eanes ED *et al*. Physicochemical evaluation of bioactive polymeric composites based on hybrid amorphous calcium phosphates. *J Biomed Mater Res* 2000; **53**(4): 381–391.
- 30 Xu HH, Moreau JL, Sun L *et al*. Nanocomposite containing amorphous calcium phosphate nanoparticles for caries inhibition. *Dent Mater* 2011; **27**(8): 762–769.
- 31 Moreau JL, Sun L, Chow LC *et al*. Mechanical and acid neutralizing properties and bacteria inhibition of amorphous calcium phosphate dental nanocomposite. *J Biomed Mater Res Part B Appl Biomater* 2011; **98**(1): 80–88.
- 32 Weir MD, Chow LC, Xu HH. Remineralization of demineralized enamel *via* calcium phosphate nanocomposite. *J Dent Res* 2012; **91**(10): 979–984.
- 33 Melo MA, Weir MD, Rodrigues LK *et al*. Novel calcium phosphate nanocomposite with caries-inhibition in a human *in situ* model. *Dent Mater* 2013; **29**(2): 231–240.



- 34 Cheng L, Weir MD, Zhang K *et al*. Antibacterial nanocomposite with calcium phosphate and quaternary ammonium. *J Dent Res* 2012; **91**(5): 460–466.
- 35 Zhou C, Weir MD, Zhang K *et al*. Synthesis of new antibacterial quaternary ammonium monomer for incorporation into CaP nanocomposite. *Dent Mater* 2013; **29**(8): 859–870.
- 36 Cheng L, Weir MD, Zhang K *et al*. Dental primer and adhesive containing a new antibacterial quaternary ammonium monomer dimethylaminododecyl methacrylate. *J Dent* 2013; **41**(4): 345–355.
- 37 Zhang K, Melo MA, Cheng L *et al*. Effect of quaternary ammonium and silver nanoparticle-containing adhesives on dentin bond strength and dental plaque microcosm biofilms. *Dent Mater* 2012; **28**(8): 842–852.
- 38 McBain AJ, Sissons C, Ledger RG *et al*. Development and characterization of a simple perfused oral microcosm. *J Appl Microbiol* 2005; **98**(3): 624–634.
- 39 Simoncic B, Tomci B. Structures of novel antimicrobial agents for textiles – a review. *Textile Res J* 2010; **80**(16): 1721–1737.
- 40 Xie D, Weng Y, Guo X *et al*. Preparation and evaluation of a novel glass-ionomer cement with antibacterial functions. *Dent Mater* 2011; **27**(5): 487–496.
- 41 Zhou H, Weir MD, Antonucci JM *et al*. Evaluation of three-dimensional biofilms on antibacterial bonding agents containing novel quaternary ammonium methacrylates. *Int J Oral Sci* 2014; **6**(2): 77–86.
- 42 Beyth N, Yudovin-Farber I, Perez-Davidi M *et al*. Polyethyleneimine nanoparticles incorporated into resin composite cause cell death and trigger biofilm stress *in vivo*. *Proc Natl Acad Sci U S A* 2010; **107**(51): 22038–22043.
- 43 Li F, Wang P, Weir MD *et al*. Evaluation of antibacterial and remineralizing nanocomposite and adhesive in rat tooth cavity model. *Acta Biomater* 2014; **10**(6): 2804–2813.
- 44 Moreau JL, Weir MD, Giuseppetti AA *et al*. Long-term mechanical durability of dental nanocomposites containing amorphous calcium phosphate nanoparticles. *J Biomed Mater Res Part B Appl Biomater* 2012; **100**(5): 1264–1273.
- 45 Alexandratos SD. Ion-exchange resins: a retrospective from industrial and engineering chemistry research. *Ind Eng Chem Res* 2009; **48**(1): 388–398.
- 46 Oh BC, Kim MH, Yun BS *et al*. Ca<sup>2+</sup>-inositol phosphate chelation mediates the substrate specificity of beta-propeller phytase. *Biochemistry* 2006; **45**(31): 9531–9539.
- 47 Griffin SO, Griffin PM, Swann JL *et al*. Estimating rates of new root caries in older adults. *J Dent Res* 2004; **83**(8): 634–638.
- 48 Banting DW, Papas A, Clark DC *et al*. The effectiveness of 10% chlorhexidine varnish treatment on dental caries incidence in adults with dry mouth. *Gerodontology* 2000; **17**(2): 67–76.
- 49 Hoppenbrouwers PM, Driessens FC, Borggreven JM. The mineral solubility of human tooth roots. *Arch Oral Biol* 1987; **32**(5): 319–322.
- 50 Keltjens H, Schaeken T, van der Hoeven H. Preventive aspects of root caries. *Int Dent J* 1993; **43**(2): 143–148.
- 51 Curzon ME, Preston AJ. Risk groups: nursing bottle caries/caries in the elderly. *Caries Res* 2004; **38**(Suppl 1): 24–33.
- 52 Lynch CD, Frazier KB, McConnell RJ *et al*. Minimally invasive management of dental caries: contemporary teaching of posterior resin-based composite placement in U.S. and Canadian dental schools. *J Am Dent Assoc* 2011; **142**(6): 612–620.



This work is licensed under a Creative Commons Attribution-NonCommercial-NoDerivs 4.0 Unported License. The images or other third party material in this article are included in the article's Creative Commons license, unless indicated otherwise in the credit line; if the material is not included under the Creative Commons license, users will need to obtain permission from the license holder to reproduce the material. To view a copy of this license, visit <http://creativecommons.org/licenses/by-nc-nd/4.0/>